Investigations of the Effect of the Non-Manganese Metal in Heterometallic-Oxido Cluster Models of the Oxygen Evolving Complex of Photosystem II: Lanthanides as Substitutes for Calcium

Po-Heng Lin, Michael K. Takase and Theodor Agapie*

Division of Chemistry and Chemical Engineering, California Institute of Technology, Pasadena, California 91125

Supporting Information

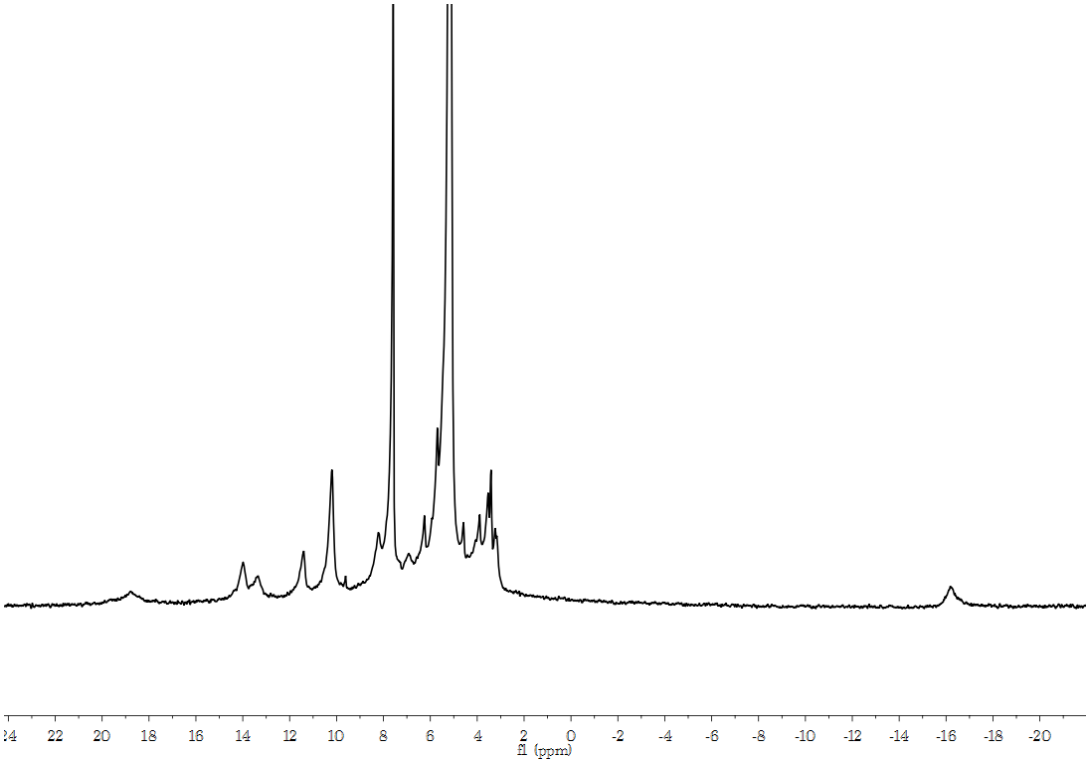

Figure S1. ^{1}H NMR spectrum of **1-La** in CD_2Cl_2 at 25 °C.

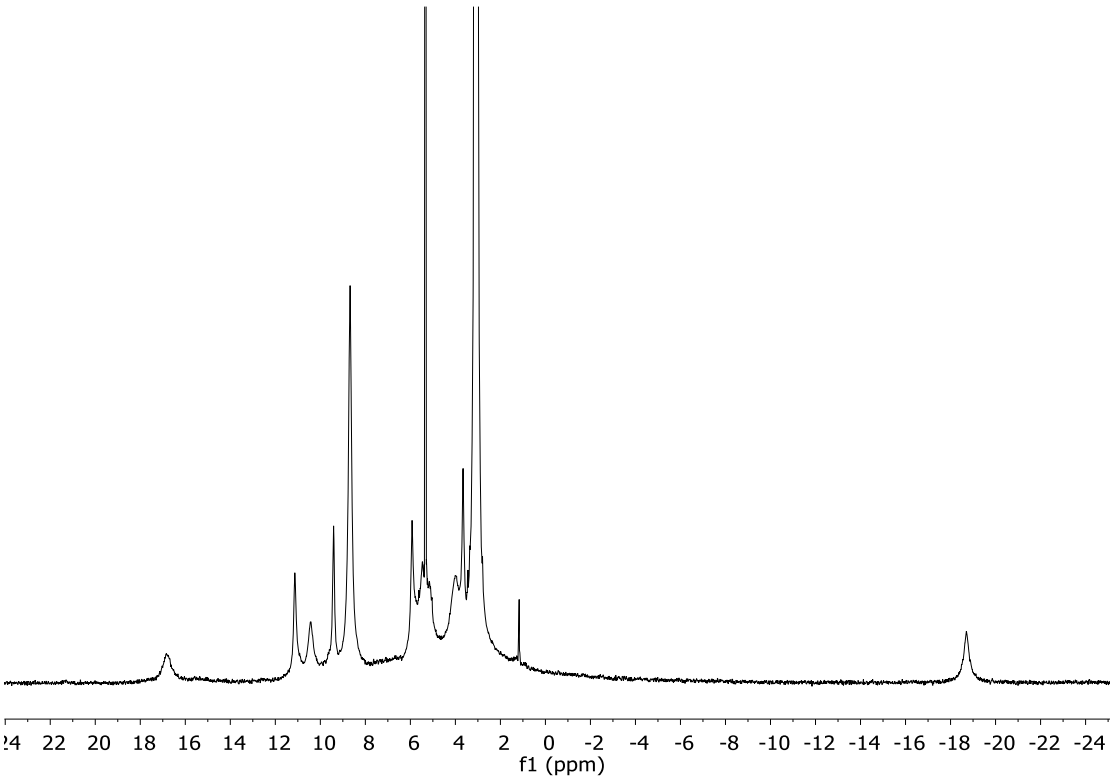

Figure S2. ^{1}H NMR spectrum of **1-Ce** in CD_2Cl_2 at 25 °C.

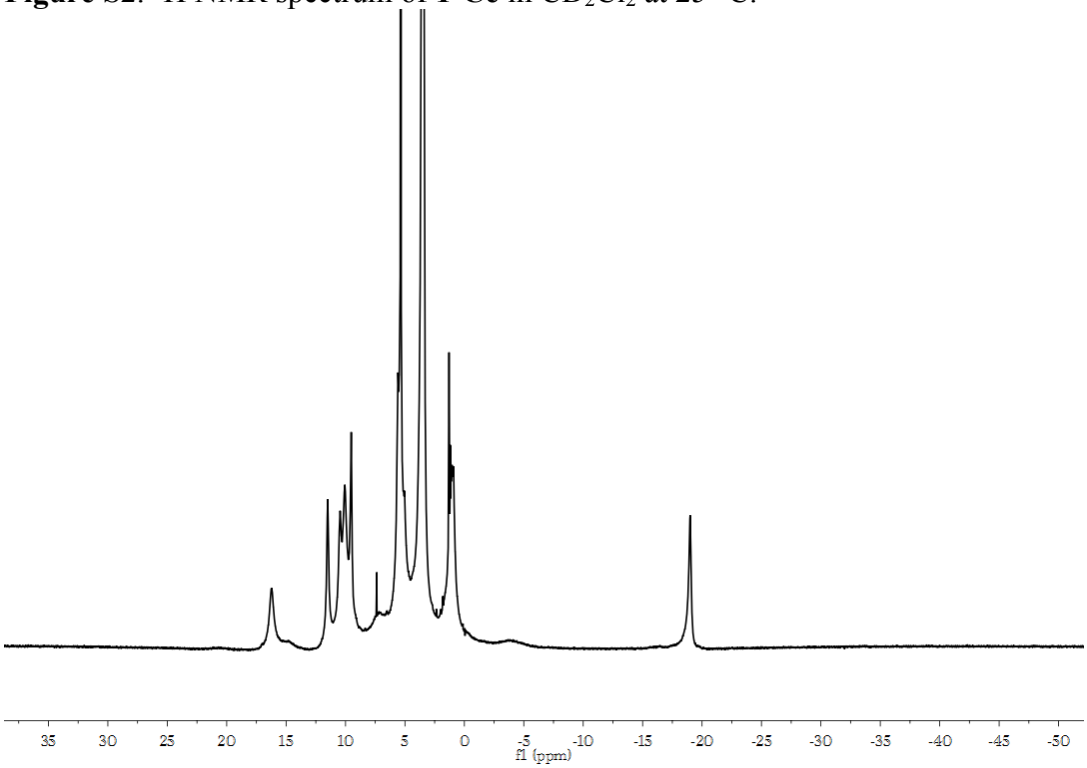

Figure S3. ^{1}H NMR spectrum of **1-Nd** in CD_2Cl_2 at 25 °C.

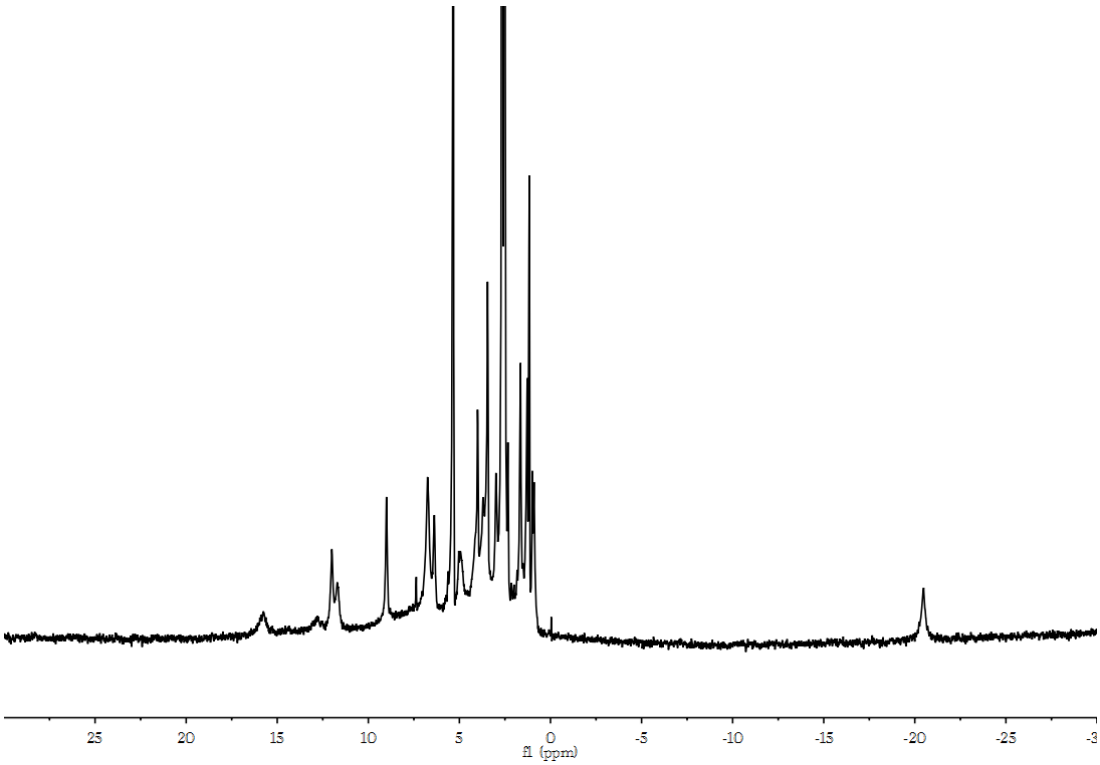

Figure S4. ^{1}H NMR spectrum of **1-Eu** in CD_2Cl_2 at 25 °C.

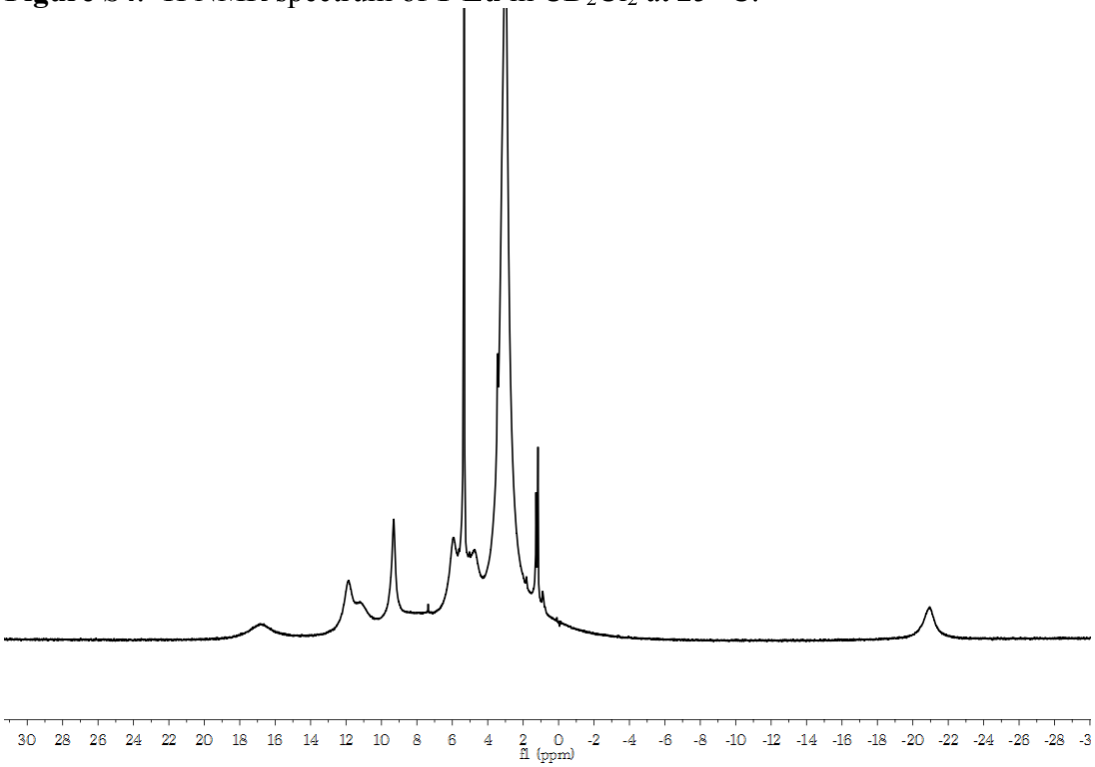

Figure S5. ^{1}H NMR spectrum of **1-Gd** in CD_2Cl_2 at 25 °C.

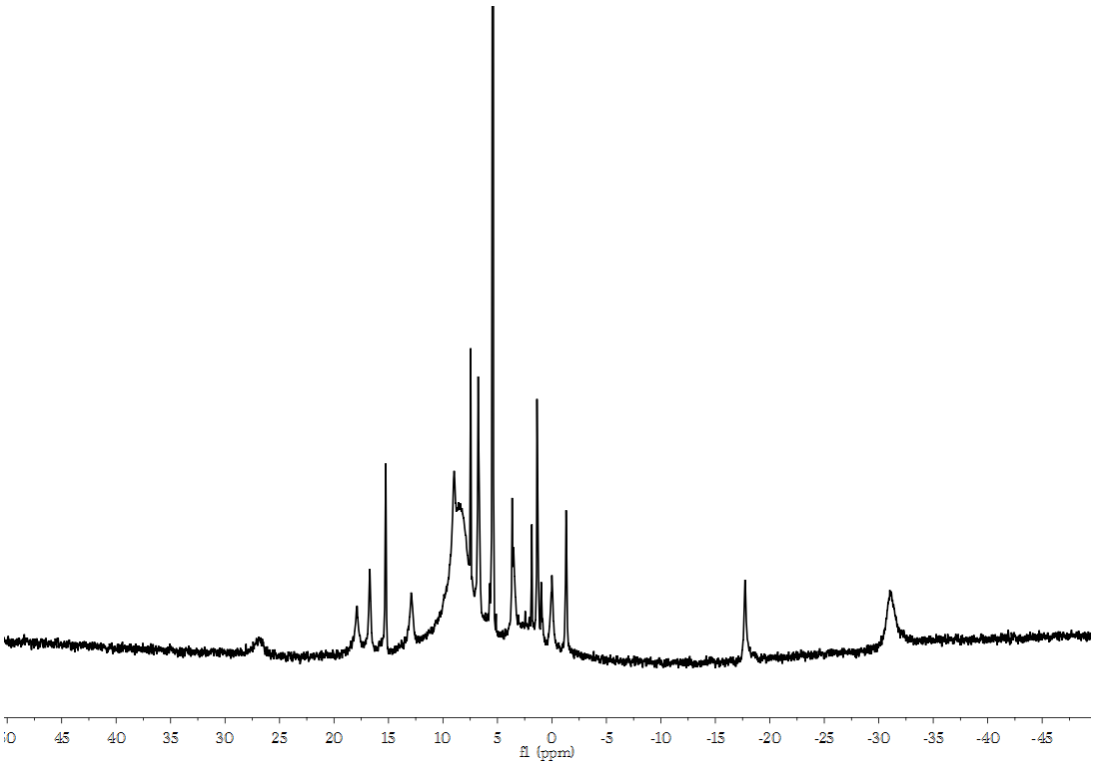

Figure S6. ^{1}H NMR spectrum of **1-Tb** in CD_2Cl_2 at 25 °C.

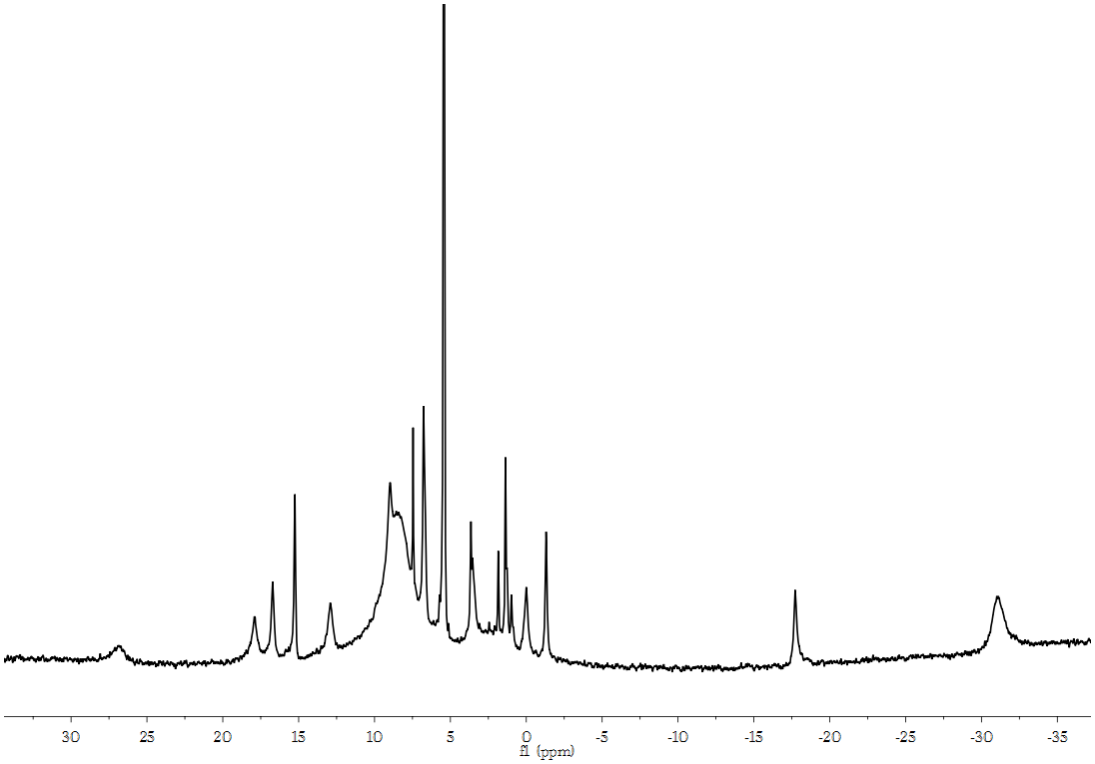

Figure S7. ^{1}H NMR spectrum of **1-Dy** in CD_2Cl_2 at 25 °C.

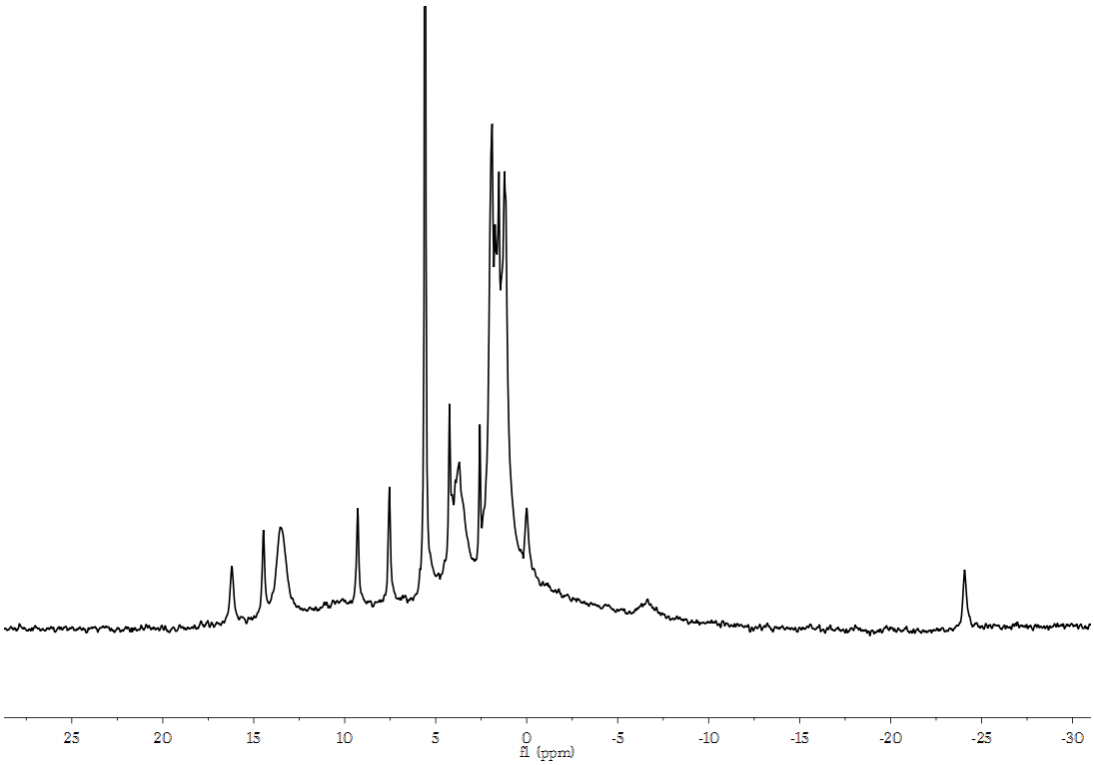

Figure S8. ^{1}H NMR spectrum of **1-Yb** in CD_2Cl_2 at 25 °C.

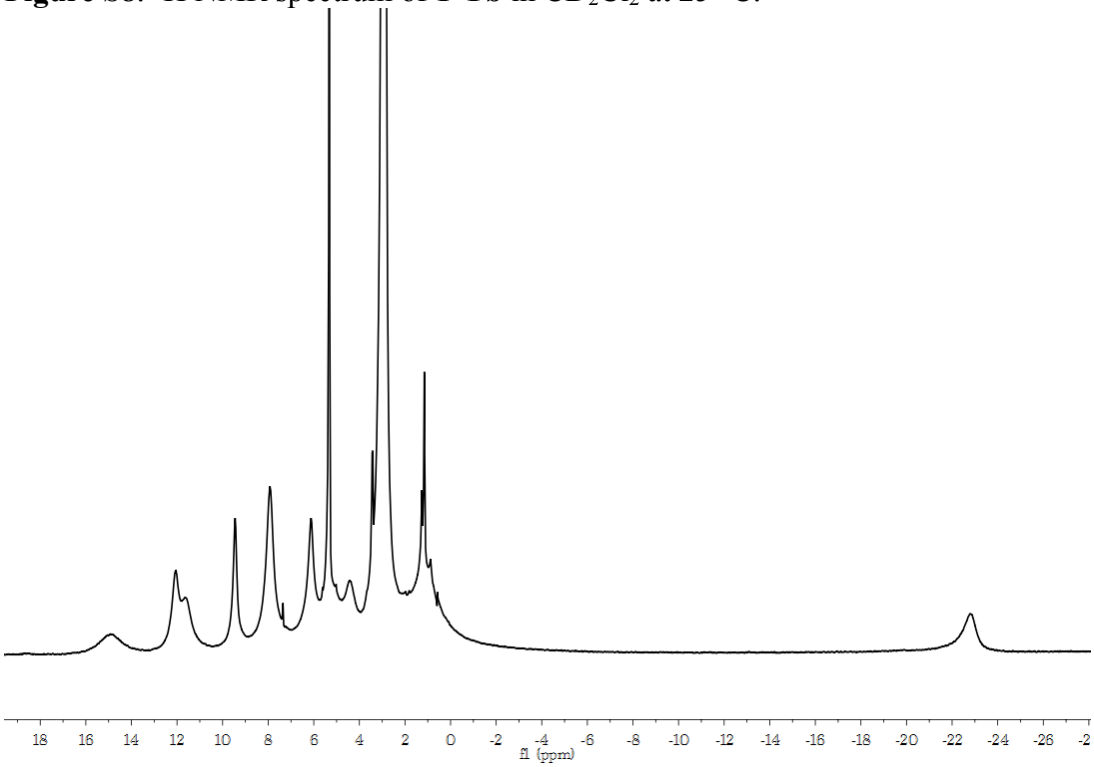

Figure S9. ^{1}H NMR spectrum of **1-Lu** in CD_2Cl_2 at 25 °C.

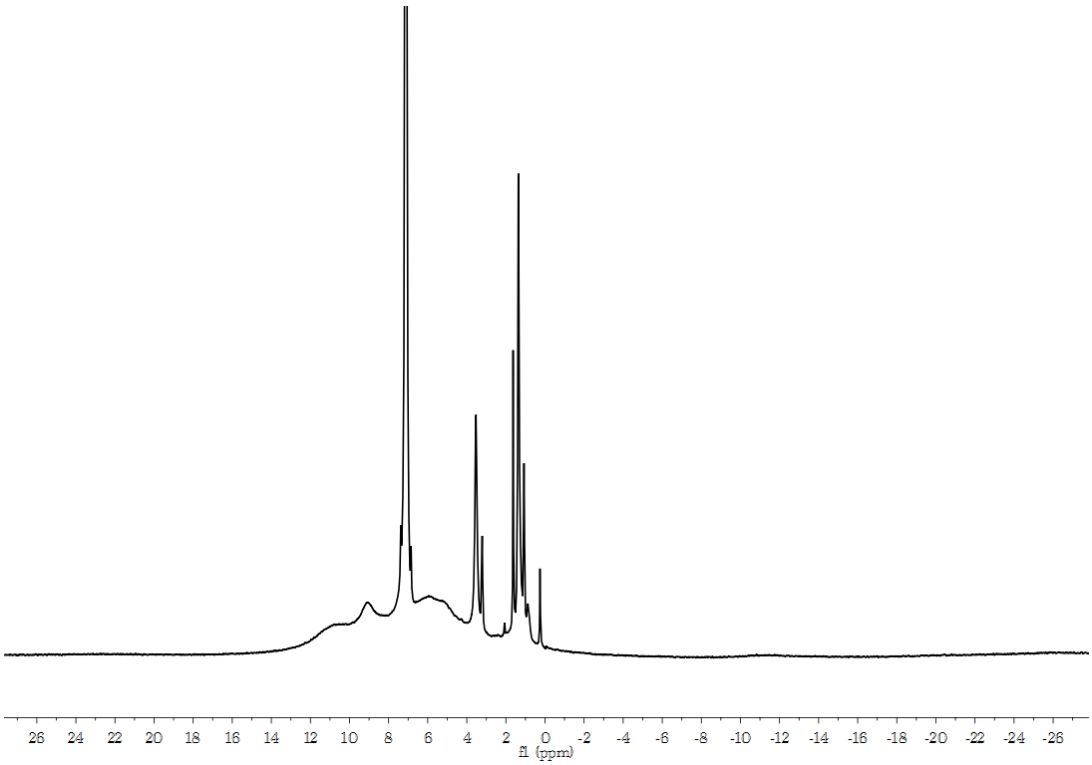

Figure S10. ^{1}H NMR spectrum of **2-Gd** in C_6D_6 at 25 °C.

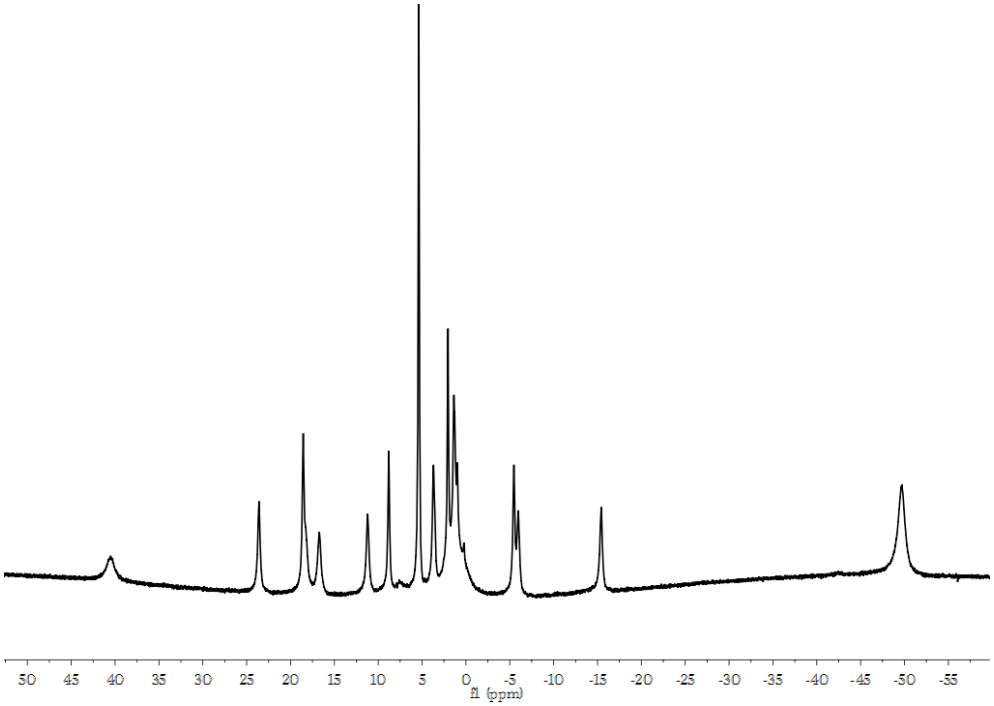

Figure S11. ^{1}H NMR spectrum of **3-Dy** in CD_2Cl_2 at 25 °C.

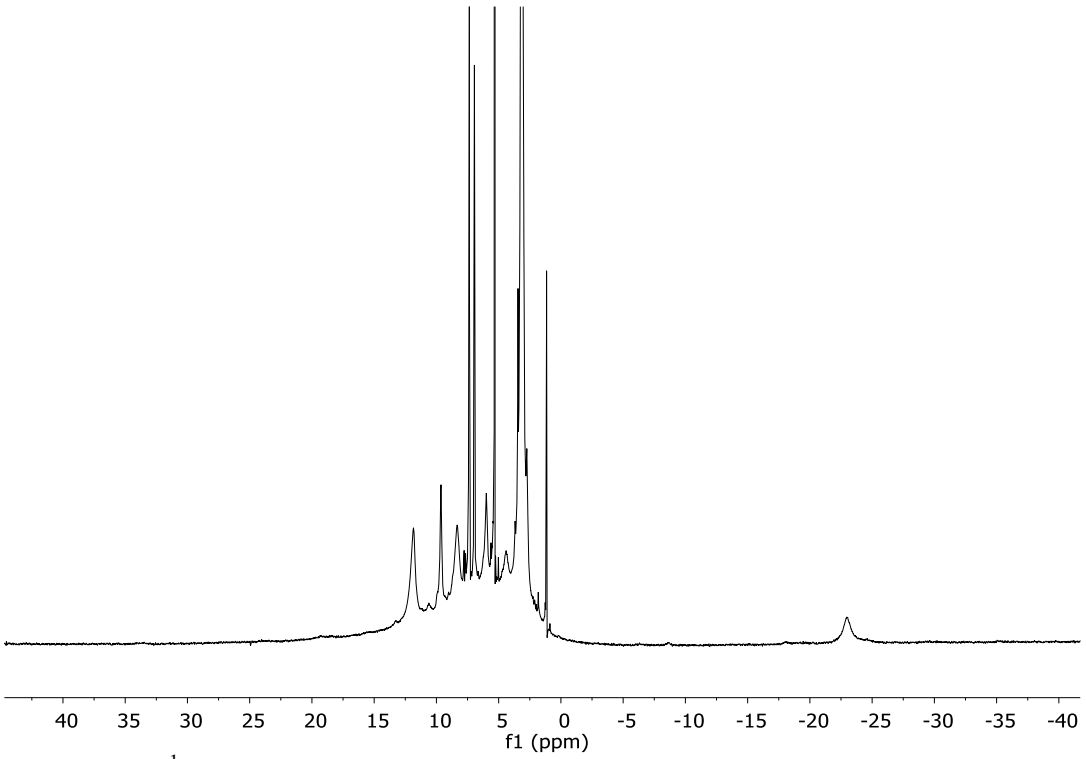

Figure S12. ^{1}H NMR spectrum of reaction of **1-Ce** with tris-(*p*-tolyl)ammoniumyl triflate (1 equiv) in CD_2Cl_2 at 25 °C.

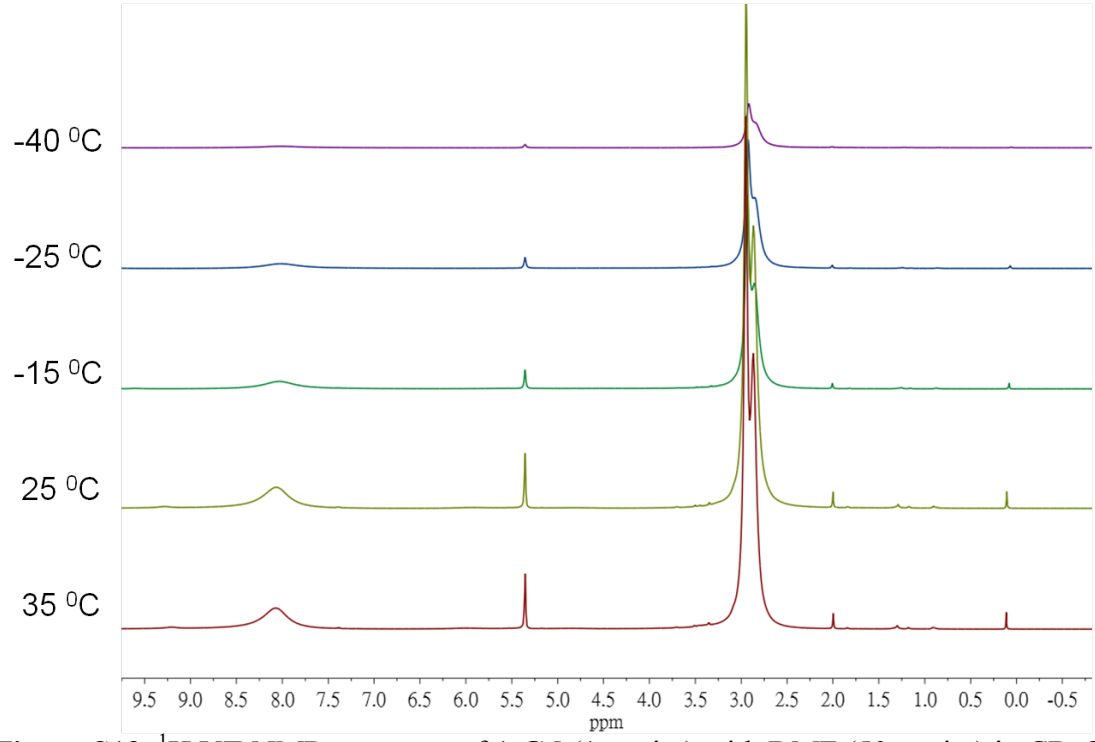

Figure S13. ^{1}H VT-NMR spectrum of **1-Gd** (1 equiv.) with DMF (50 equiv.) in CD_2Cl_2 between 35 to -40 °C. Only one set of peaks (8.1 and 2.9 ppm) corresponding to DMF was observed in the NMR spectrum even at -40 ^{0}C.

Cyclic Voltammetry

Electrochemical measurements of *ca.* 1 mM solutions of the relevant complexes were recorded in the glovebox at 20 °C using a Pine Instrument Company AFCBP1 bipotentiostat, an auxiliary Pt-coil electrode, a Ag/Ag^+ reference electrode (0.01M $AgNO_3$ in CH_3CN), and a 3.0 mm glassy carbon electrode disc (BASI). The electrolyte solution was 0.1 M $^nBu_4NPF_6$ in Dimethylacetamide(DMA). Data were recorded using the Pine Instrument Company AfterMath software package. All reported values are referenced to an internal ferrocene/ferrocenium couple (Fc/Fc^+).

Table S1. Reduction potentials of $[LnMn_3O_4]$ complexes. Potentials were referenced to Fc/Fc^+.

	1-La	**1-Ce**	**1-Nd**	**1-Eu**	**1-Gd**	**1-Tb**	**1-Dy**	**1-Yb**	**1-Lu**
$E_{1/2}$ (V)	-0.49	-0.46	-0.44	-0.43	-0.43	-0.41	-0.41	-0.38	-0.35

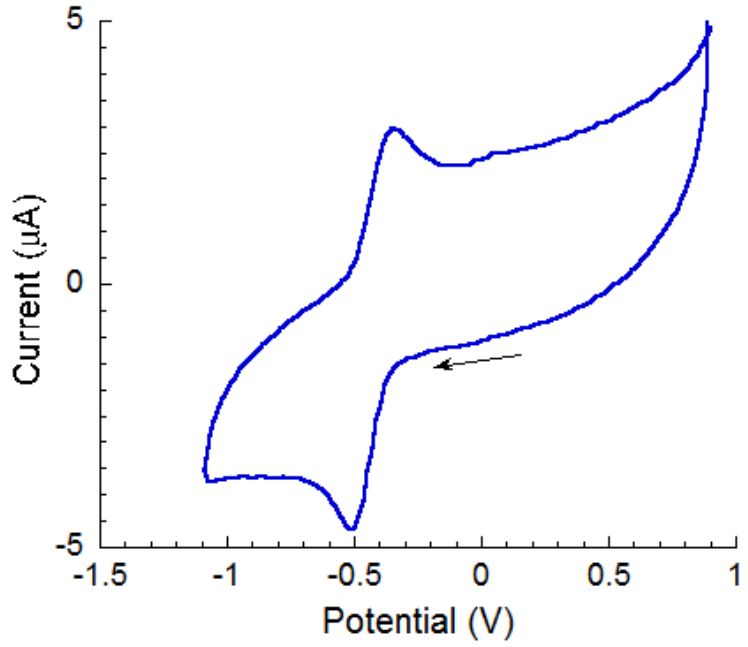

Figure S14. Cyclic voltammogram of **1-Nd** in 0.1 M NBu_4PF_6 in DMA using a glassy carbon disc electrode. Scan rate of 100 mV/s. Potentials are referenced to Fc/Fc^+.

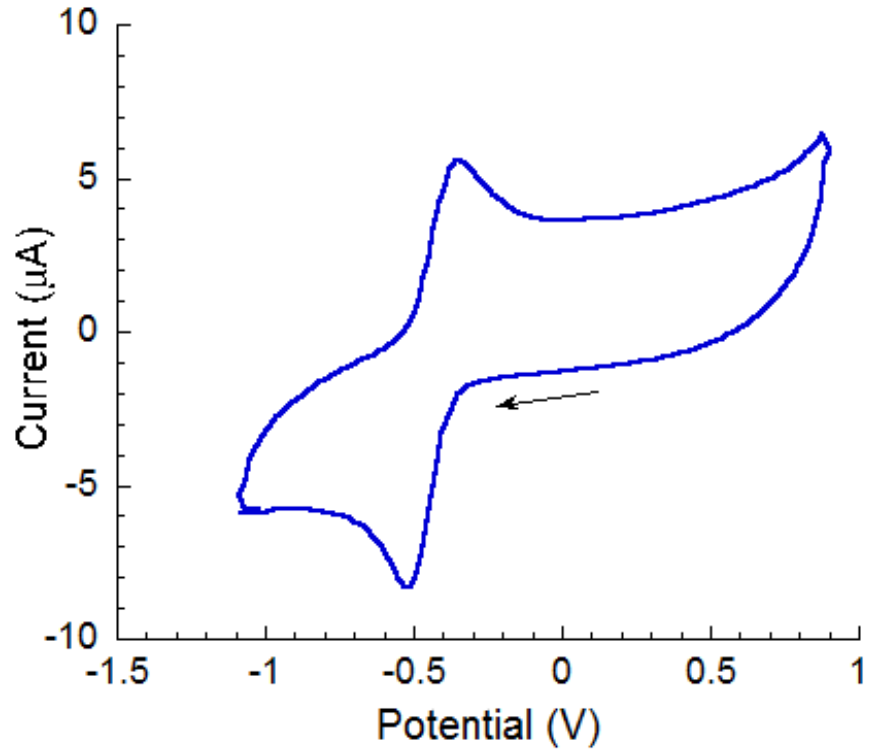

Figure S15. Cyclic voltammogram of **1-Eu** in 0.1 M NBu_4PF_6 in DMA using a glassy carbon disc electrode. Scan rate of 100 mV/s. Potentials are referenced to Fc/Fc^+.

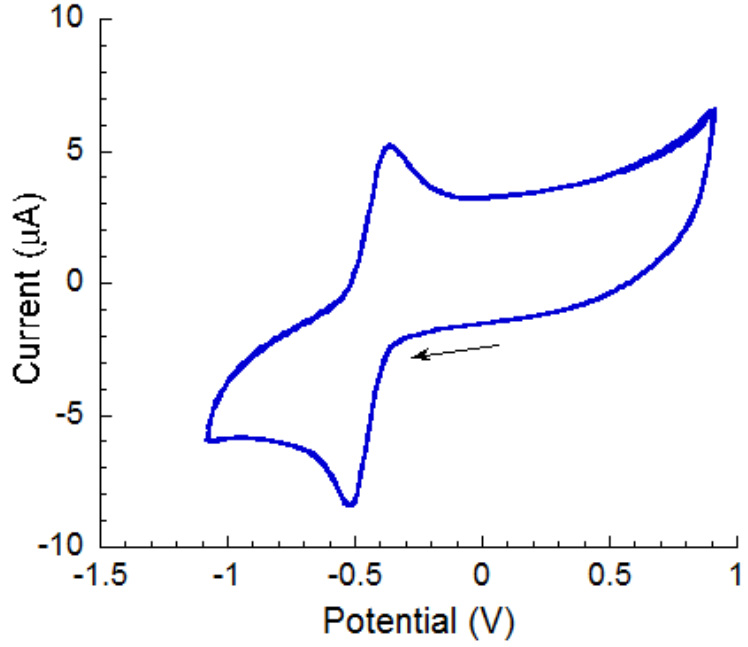

Figure S16. Cyclic voltammogram of **1-Gd** in 0.1 M NBu_4PF_6 in DMA using a glassy carbon disc electrode. Scan rate of 100 mV/s. Potentials are referenced to Fc/Fc^+.

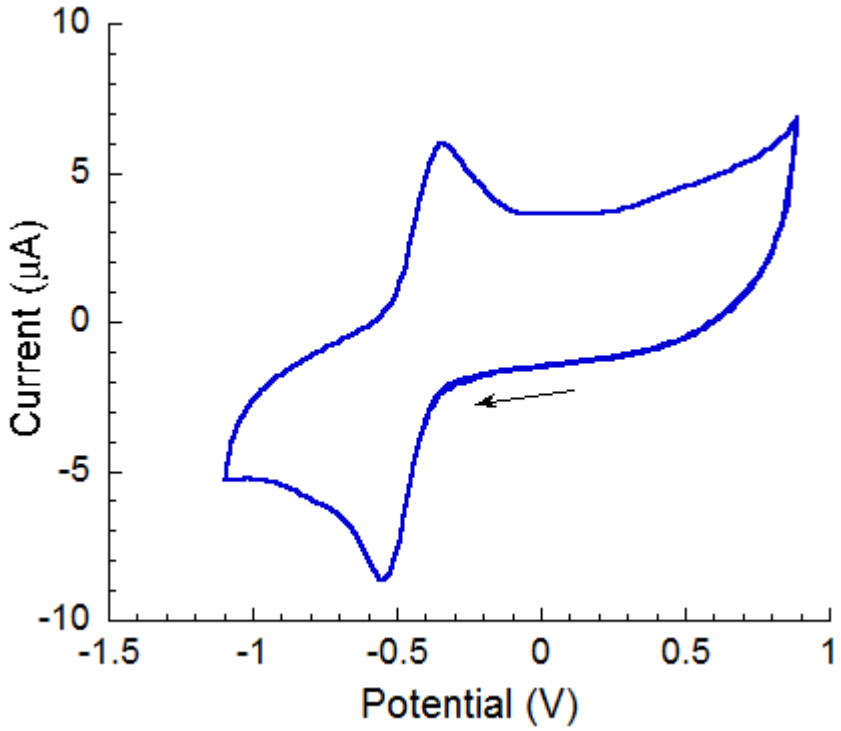

Figure S17. Cyclic voltammogram of **1-Tb** in 0.1 M NBu_4PF_6 in DMA using a glassy carbon disc electrode. Scan rate of 100 mV/s. Potentials are referenced to Fc/Fc^+.

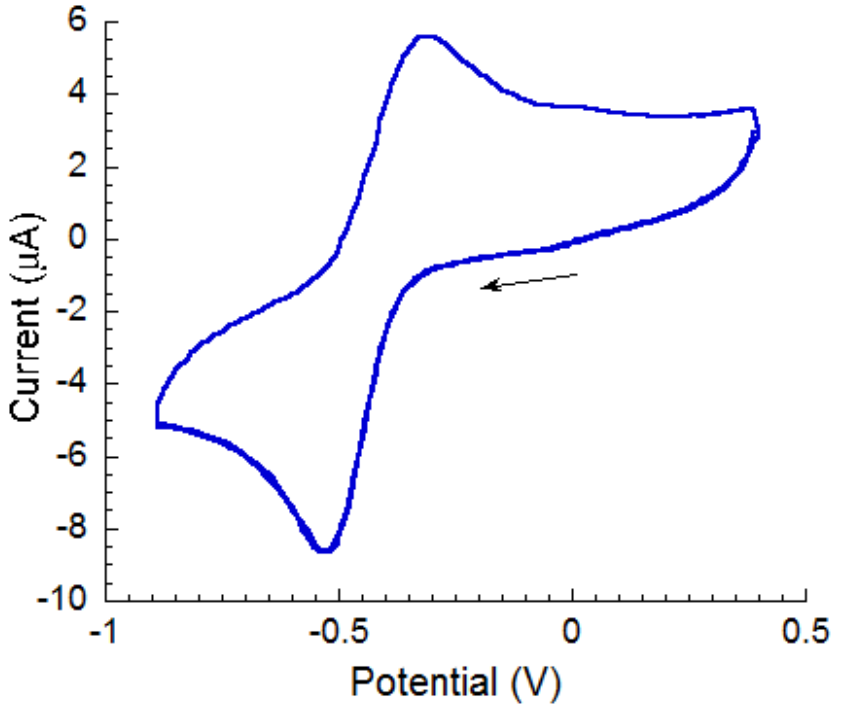

Figure S18. Cyclic voltammogram of **1-Dy** in 0.1 M NBu_4PF_6 in DMA using a glassy carbon disc electrode. Scan rate of 100 mV/s. Potentials are referenced to Fc/Fc^+.

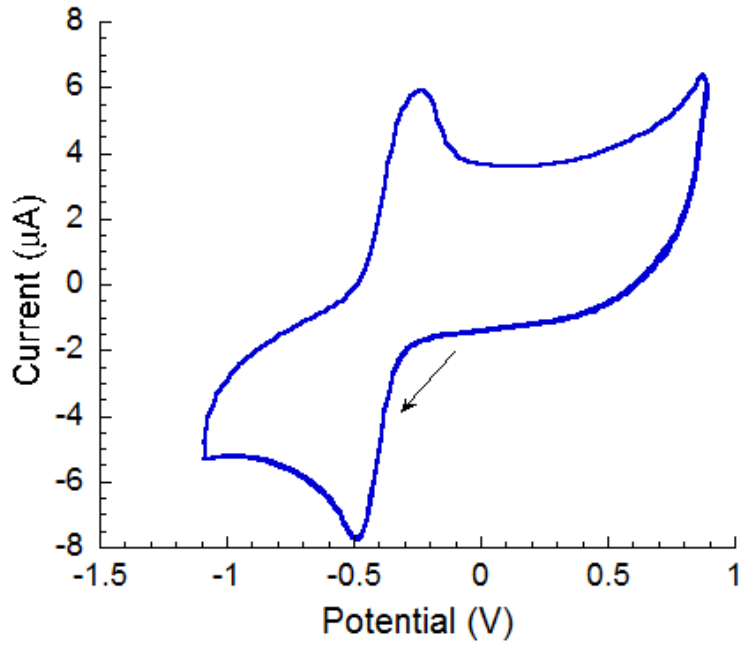

Figure S19. Cyclic voltammogram of **1-Yb** in 0.1 M NBu_4PF_6 in DMA using a glassy carbon disc electrode. Scan rate of 100 mV/s. Potentials are referenced to Fc/Fc^+.

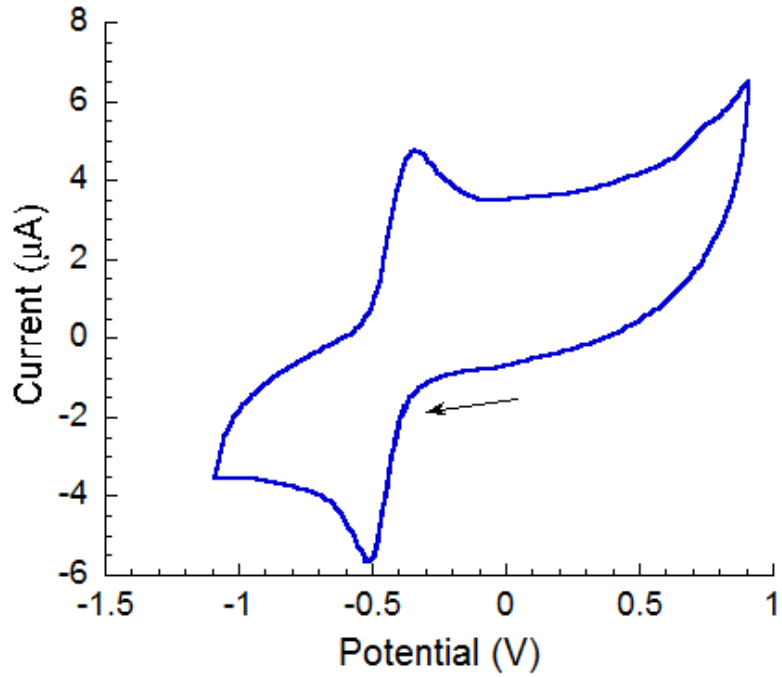

Figure S20. Cyclic voltammogram of **2-Gd** in 0.1 M NBu_4PF_6 in DMA using a glassy carbon disc electrode. Scan rate of 100 mV/s. Potentials are referenced to Fc/Fc^+.

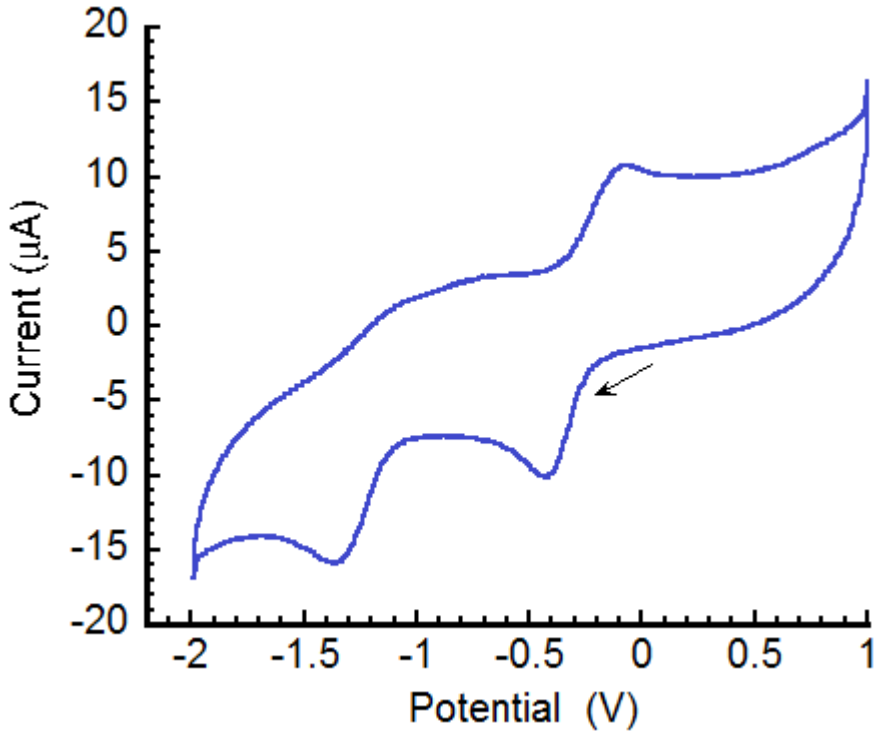

Figure S21. Cyclic voltammogram of **1-Lu** in 0.1 M NBu_4PF_6 in DMA using a glassy carbon disc electrode. Scan rate of 250 mV/s. Potentials are referenced to Fc/Fc^+.

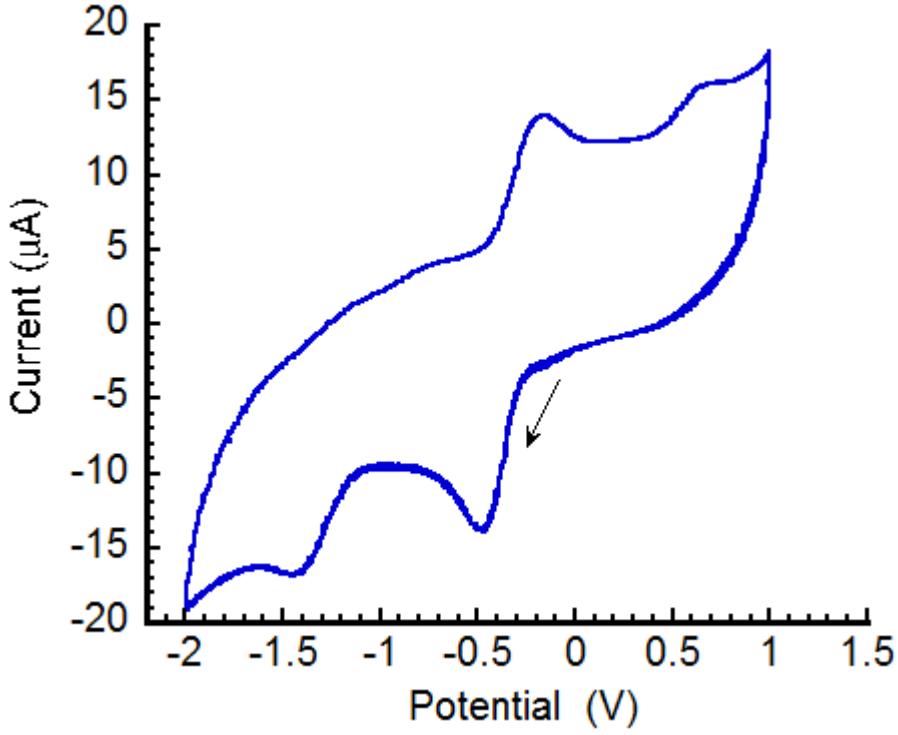

Figure S22. Cyclic voltammogram of **1-Tb** in 0.1 M NBu_4PF_6 in DMA using a glassy carbon disc electrode. Scan rate of 250 mV/s. Potentials are referenced to Fc/Fc^+.

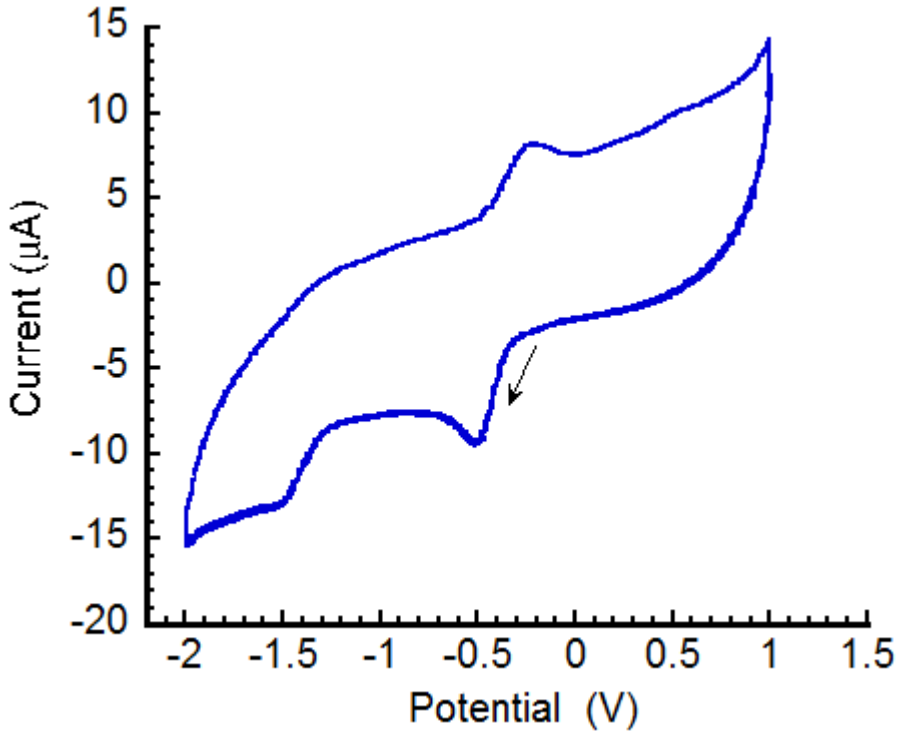

Figure S23. Cyclic voltammogram of **1-La** in 0.1 M NBu_4PF_6 in DMA using a glassy carbon disc electrode. Scan rate of 250 mV/s. Potentials are referenced to Fc/Fc^+.

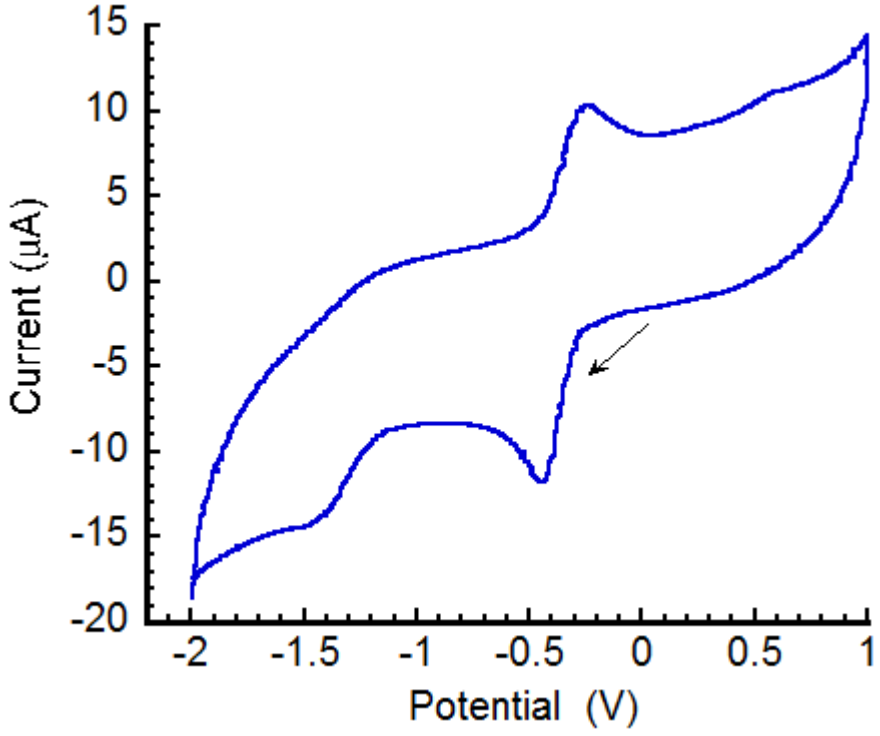

Figure S24. Cyclic voltammogram of **1-Gd** in 0.1 M NBu_4PF_6 in DMA using a glassy carbon disc electrode. Scan rate of 250 mV/s. Potentials are referenced to Fc/Fc^+.

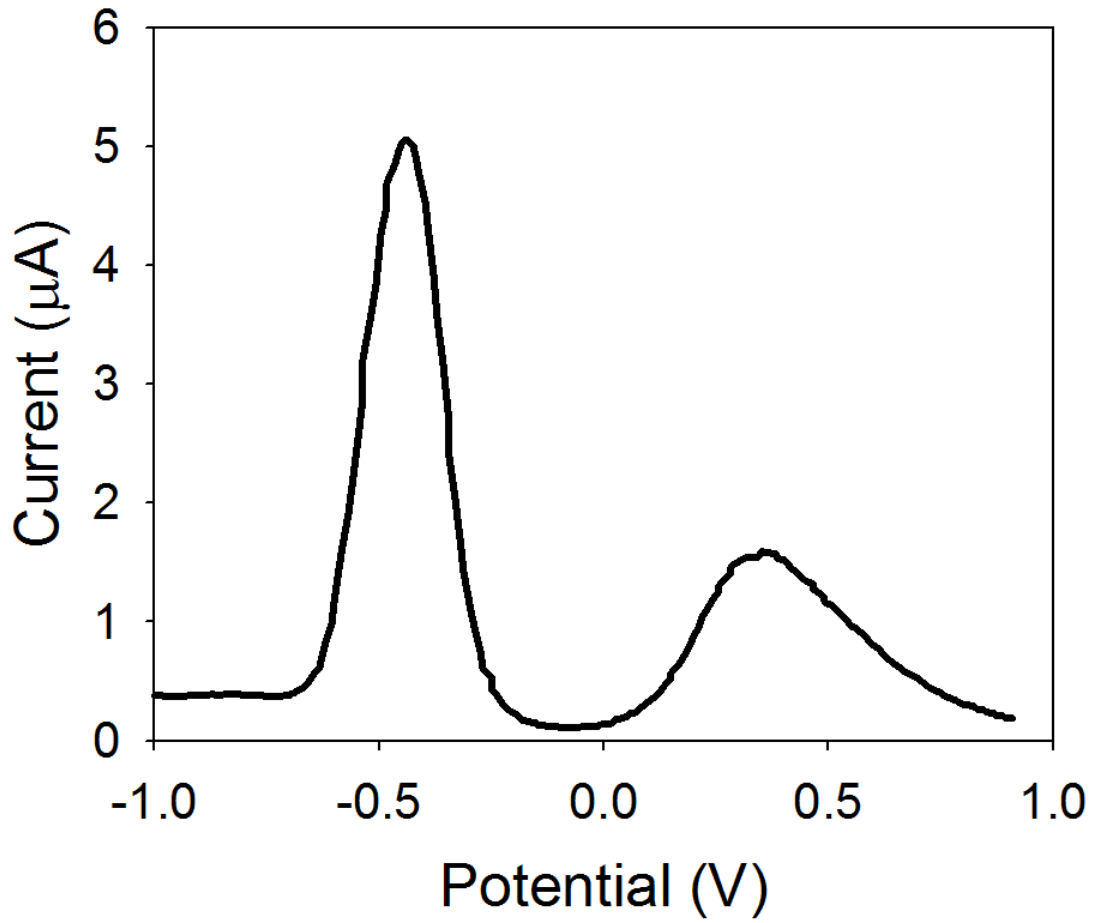

Figure S25. Square-wave voltammogram of **1-Ce** in 0.1 M NBu_4PF_6 in DMA with 100 mV square amplitude and 10 mV square increment. Potentials are referenced to Fc/Fc^+. Ratio of area under the peaks is 0.7.

Crystallographic Information

CCDC 1010437-1010441 contain the supplementary crystallographic data for this paper. These data can be obtained free of charge from The Cambridge Crystallographic Data Centre via www.ccdc.cam.ac.uk/data_request/cif.

Low-temperature diffraction data (ϕ-and ω-scans) were collected on a Bruker Kappa diffractometer coupled to a Apex II CCD detector with graphite monochromated Mo K_α radiation (λ = 0.71073 Å) for the structure of compounds **1-Yb**, **1-Gd**, **1-La**, and **2-Gd** and at Beamline 12-2 at the Stanford Synchrotron Radiation Lightsource (SSRL, λ = 0.72930 Å, Dectris Pilatus 6M detector) for the structure of compound **3-Dy**. The structures were solved by direct methods using SHELXS[1] and refined against F^2 on all data by full-matrix least squares with

SHELXL-2014[2] using established refinement techniques.[3] All non-hydrogen atoms were refined anisotropically. All hydrogen atoms were included into the model at geometrically calculated positions and refined using a riding model. The isotropic displacement parameters of all hydrogen atoms were fixed to 1.2 times the *U* value of the atoms they are linked to (1.5 times for methyl groups). All disordered atoms were refined with the help of similarity restraints on the 1,2- and 1,3-distances and displacement parameters as well as rigid bond restraints for anisotropic displacement parameters.

Compound **1-Yb** crystallizes in the triclinic space group *P*-1 with one molecule in the asymmetric unit along with one triflate anion and two dimethylformamide molecules. The triflate anion was disordered over two positions. The thermal ellipsoids are elongated in the disordered model indicating additional unrefined disorder, however, additional components could not be successfully refined.

Compound **1-Gd** crystallizes in the triclinic space group *P*-1 with one molecule in the asymmetric unit along with one triflate anion and two molecules of dimethylformamide. The triflate anion was disordered over three mutually exclusive positions. The occupancy of the three components refined to 0.619(2):0.224(2):0.157(2). Two of the dimethylformamide molecules, one bound to the gadolinium atom and one outer sphere, were disordered over two positions. The occupancy of the two components refined to 0.740(5):0.260(5) and 0.804(5):0.196(5) for the inner sphere and outer sphere dimethylformamide molecules, respectively.

Compound **1-La** crystallizes in the monoclinic space group R-3 with 1/3 of a molecule in the asymmetric unit along with 1/3 of a triflate anion and 1/3 of a dimethylformamide. The dimethylformamide was refined with the help of similarity restraints on the 1,2- and 1,3-distances and displacement parameters as well as enhanced rigid bond restraints for anisotropic displacement parameters. All five atoms of the dimethylformamide were restrained to line in a plane. The crystal was twinned with twin law (-1 -1 0, 0 1 0, 0 0 -1). The twin ratio was refined freely and converged at 0.1582(5). In addition, the structure contained a solvent accessible void which could not be modeled. The program SQUEEZE[4] as implemented in Platon[5] was used to remove the contribution of the disordered solvent to the structure factors.

Compound **2-Gd** crystallizes in the monoclinic space group $P2_1/n$ with one molecule in the asymmetric unit along with one molecule of benzene as well as a mixture of 1.048 dimethylformamide and 1.476 diethyl ether molecules, disordered over five independent positions. The occupancy of one diethyl ether and two dimethylformamide molecules refined to 0.524(2). The occupancy of the other two, mutually exclusive, ether molecules refined to 0.476(2).

Compound **3-Dy** crystallizes in the triclinic space group *P*-1 with one molecule in the asymmetric unit along with one triflate anion, two water, and one acetonitrile molecules. The triflate anion was modeled as a three component disorder. The three, mutually exclusive, components were refined with the help of similarity restraints on the 1,2- and 1,3-distances and displacement parameters as well as enhanced rigid bond restraints for anisotropic displacement parameters. The occupancy of the three components refined to 0.502(2):0.274(3):0.224(3). Additional residual electron density is located near the triflate molecules indicating additional disorder, however, refinement of additional components was not successful. The hydrogen atoms on the two water molecules bound to the dysprosium atom could be observed in the difference Fourier synthesis, but could not be refined. The hydrogen atoms on the two outer sphere water molecules could not be found. All water hydrogen atoms were not included into the model.

Table S2. Crystal and refinement data for reported complexes

	1-Gd	1-La	1-Yb	2-Gd	3-Dy
empirical formula	C76 H76 F3 Gd Mn3 N10 O20 S	C76 H76 F3 La Mn3 N10 O20 S	C76 H77 F3 Mn3 N10 O20 S Yb	C83.95 H89.90 Gd Mn3 N8.95 O17.48	C66 H59 Dy F3 Mn3 N7 O20 S
formula wt	1860.59	1842.25	1877.38	1825.98	1686.58
T (K)	100	100	100	100	100
a, Å	12.9591(6)	14.3292(5)	12.9443(7)	17.8990(7)	14.360(3)
b, Å	14.9868(7)	14.3292(5)	14.9826(9)	16.8266(6)	14.690(3)
c, Å	19.8869(9)	67.288(3)	19.8350(10)	27.7628(10)	17.010(3)
α, deg	84.749(3)	90	84.470(3)	90	106.08(3)
β, deg	81.986(3)	90	82.046(3)	108.026(2)	101.08(3)
γ, deg	87.662(3)	120	87.539(3)	90	94.65(3)
V, $Å^3$	3807.0(3)	11965.0(10)	3790.3(4)	7951.2(5)	3349.1(13)
Z	2	6	2	4	2
cryst syst	Triclinic	Trigonal	Triclinic	Monoclinic	Triclinic
space group	P-1	R-3	P-1	$P2_1/n$	P-1
d_{calcd}, g/cm^3	1.623	1.534	1.644	1.525	1.672
θ range, deg	2.064 -29.130	2.039-45.320	2.014-30.573	1.206-36.360	1.312-31.393
μ, mm^{-1}	1.461	1.099	1.826	1.365	1.887
abs cor	Semi-empirical from equivalents	Semi-empirical from equivalents	Semi-empirical from equivalents	Semi-empirical from equivalents	Semi-empirical from equivalents
GOF[c]	1.027	1.118	1.008	1.041	1.047
R1,[a] wR2[b] (I > 2σ(I))	0.0780, 0.0843	0.0525, 0.1034	0.0835, 0.793	0.0390, 0.0647	0.0469, 0.1306

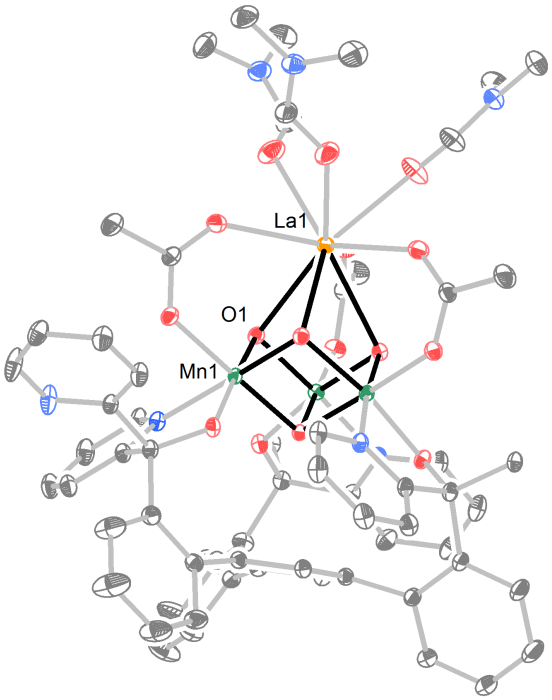

Figure S26. The molecular X-ray structures of **1-La** with the ellipsoids drawn at the 50% probability level. Hydrogen atoms have been removed for clarity.

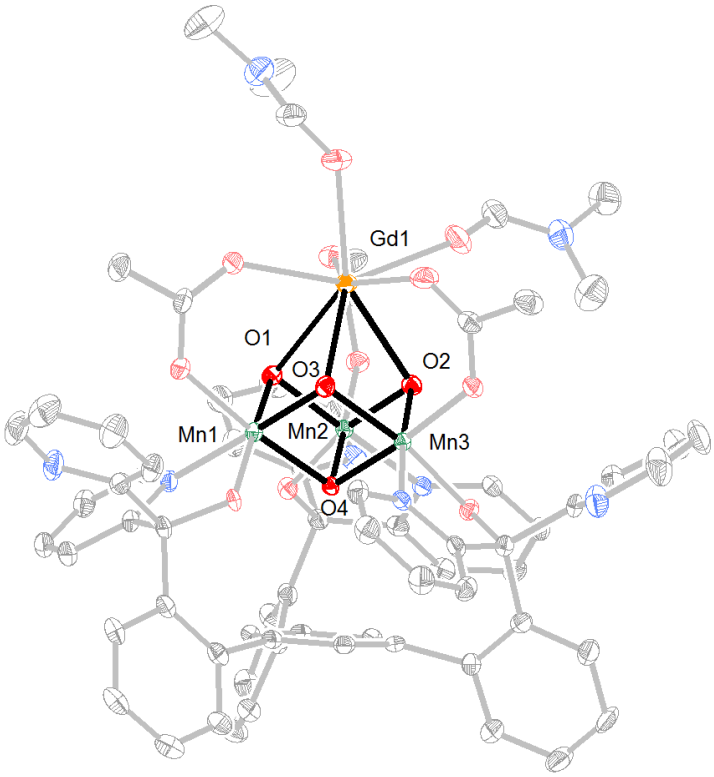

Figure S27. The molecular X-ray structures of **1-Gd** with the ellipsoids drawn at the 50% probability level. Hydrogen atoms have been removed for clarity.

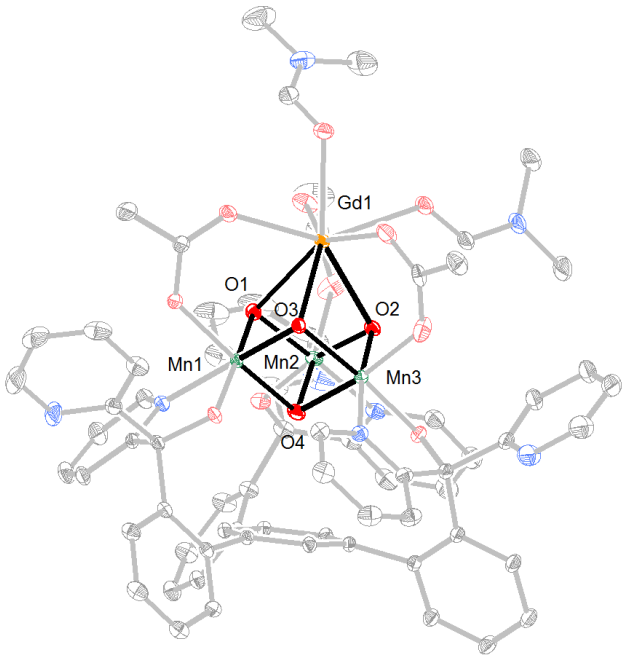

Figure S28. The molecular X-ray structures of **2-Gd** with the ellipsoids drawn at the 50% probability level. Hydrogen atoms have been removed for clarity.

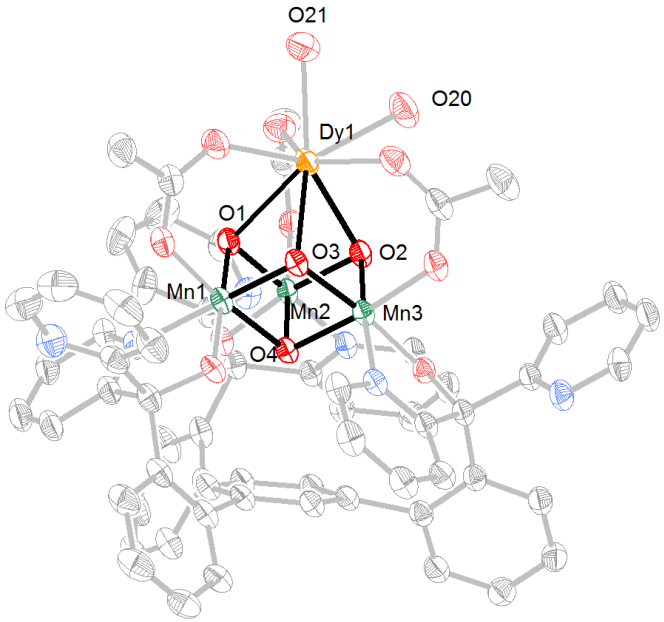

Figure S29. The molecular X-ray structures of **3-Dy** with the ellipsoids drawn at the 50% probability level. Hydrogen atoms have been removed for clarity.

---

[1] Sheldrick, G. M. *Acta Cryst.* **1990**, A46, 467-473.

[2] Sheldrick, G. M. *Acta Cryst.* **2008**, A64, 112-122.

[3] Müller, P. *Crystallography Reviews* **2009**, *15*, 57-83.

[4] van der Sluis, P.; Spek, A. L. *Acta Cryst.* **1990**, A46, 194–201.

[5] Spek, A. L. *Acta Cryst.* **2009**, D65, 148–155.